Characteristic Energy Loss of Electrons Passing Through Metal Foils: Momentum-Exciton Model of Plasma Oscillations*†

RICHARD A. FERRELL AND JOHN J. QUINN
University of Maryland, College Park, Maryland
(Received July 11, 1957)

Previous work is extended so as to obtain a unified theory of collective and individual electron effects in the excitation of a degenerate electron gas by fast incident electrons. The two characteristically collective features of the characteristic energy loss, the relatively large magnitude and the sharpness of the energy, are shown to follow from a straightforward quantum-mechanical treatment of one-electron excitations, provided only that the interactions of the electrons are taken into account. The interaction causes the excitation to be transferred from one excited configuration to another, resulting in an exciton in momentum space. This "momentum-exciton" is a discrete state which separates from the continuum of one-electron excitations and rises to higher energy, in accordance with Hund's rule. Correlation is taken into account by means of Feynman graphs in which the excitation makes a "jog" and travels backwards in time, as well as forwards. With this refinement the identification of the momentum-exciton with the Bohm-Pines plasma oscillation is completed.

I. INTRODUCTION

As emphasized in Sec. III of I, there are two qualitative features of the inelastic scattering of fast electrons by metal foils which are impossible to understand on the basis of individual excitation of noninteracting conduction electrons. These are first, the magnitude of the energy loss, which is much greater than the change in kinetic energy which the conduction electrons experience upon being excited out of the Fermi sea, at least for small angles of scattering. The second feature is the sharpness of the characteristic energy loss, or eigenloss as we prefer to call it, which bears no resemblance to the broad low-lying continuum of kinetic energy increments. The failure of this simple theory is clearly attributable to the neglect of the Coulomb interactions between pairs of electrons. The main effect of the interactions is to permit plasma oscillations, which in turn immediately explain away the above two discrepancies. In I the plasma oscillations were treated in the style of the Bohm-Pines theory by introducing collective coordinates. Since it is permitted to introduce only a limited number of these coordinates, it is not possible to handle all of the inelastic scattering in this way. This treatment therefore suffered from the unsatisfactory feature that at a certain maximum angle of scattering it was necessary to "switch over" from Bohm-Pines theory to one-electron theory. The first step in developing a more unified approach was made in II, where the excitation of plasma oscillations was described quantitatively without the introduction of collective variables. In this time-dependent self-consistent field treatment it was necessary to work in the classical limit of large quantum numbers of excitation for the plasma oscillators, and to invoke the *correspondence principle* in order to obtain relations for plasmon creation in the ground state.

The present paper has as its purpose first to establish that all of the results obtained in II can be verified directly without the necessity of working in the classical limit. In addition the magnitude of the eigenloss as well as its sharpness are shown to follow from a straightforward quantum-mechanical treatment of one-electron excitation, *provided* the Coulomb interactions of the electrons are taken into account. One finds that a plasma oscillation is nothing but an exciton in momentum space. An electron excited out of the Fermi sea can interact with another electron and excite it, with the first electron at the same time falling back into its hole. In this way the excitation is passed about in momentum space from one electron to another. The stationary state representing a plasmon is simply a certain linear combination of the various one-electron excitations. The collective nature of the plasmon arises from the fact that such a superposition can have properties different from those of the individual basis states.

In Sec. II we evaluate the total interaction energy belonging to the superposition generated by the scattering itself. This is seen to account quite adequately for the magnitude of the eigenloss. In addition the electron-electron positional correlation resulting from this configuration mixing is exhibited explicitly. In Sec. III the interaction of the one-electron excitations is studied in more detail and by means of a sort of Tamm-Dancoff treatment an approximate diagonalization of the Hamiltonian is carried out. As the interaction strength is increased from zero, at first no qualitative change occurs in the spectrum of excited states. But after the strength surpasses a certain minimum value, a discrete state splits off from the continuum of one-electron excitations and rises to considerably higher energies as the interaction strength is further increased. This "momentum-exciton" is

* Investigation supported by the Office of Naval Research.
† Preliminary report: J. J. Quinn and R. A. Ferrell, Bull. Am. Phys. Soc. Ser. II, 1, 44 (1956). The present paper constitutes a continuation of already published work which will be referred to to as I [R. A. Ferrell, Phys. Rev. **101**, 554 (1956)], and II [R. A. Ferrell, Phys. Rev. **107**, 450 (1957)].

identical to a plasmon, within the approximations inherent in the Tamm-Dancoff treatment. The refinements necessary to complete this identification are made in Sec. IV. The effects of three-, five-, etc., electron excitations in the excited state and two-, four-, etc., electron excitations in the ground state must be taken into account. It is not necessary to calculate the energies of the two states separately since all we are interested in at present is their difference. The difference is most easily calculated by using the Feynman time-dependent formulation of the Schrödinger equation. "Bubble" graphs cancel out of the difference, leaving only irreducible graphs in which the excitation makes a "jog" and travels backwards in time, as well as forwards. Inclusion of such graphs completes the identification of the momentum-exciton with the plasmon. In this way all the results of II can be verified directly for plasmon creation in the ground state. A brief summary constitutes Sec. V.

II. INTERACTION ENERGY

The first goal of this paper is to demonstrate how an interacting degenerate electron gas can absorb from an incident electron very much more energy than can be accounted for in terms of individual kinetic-energy increments. Suppose the incident electron undergoes a change of momentum $-\hbar\mathbf{k}$. Figure 2 of I shows the fraction of the Fermi sea which is permitted by the Pauli exclusion principle to undergo one-electron excitation. The kinetic-energy increments corresponding to these one-electron excitations form a continuum whose maximum equals $(\hbar^2/2m)(k^2+2kk_0)$, where $\hbar k_0$ is the Fermi momentum and m the electron mass. This continuum is illustrated in Fig. 1 of II. It is completely inadequate, for small momentum transfer, to account for the relatively large energy losses observed (e.g., 15 ev in aluminum). In the extreme case of $k\rightarrow 0$ the continuum contracts to zero. One is forced to attribute the discrepancy to the interaction of the electrons, which, of course, should be taken into account anyway.

For the present qualitative purposes of this section let us therefore calculate the total potential energy of the state generated by the scattering of the incident electron. According to Sec. III of I, the incident electron acts on the Slater determinant representing the unperturbed Fermi sea by means of the operator $\sum_i e^{i\mathbf{k}\cdot\mathbf{x}_i}$, where $\mathbf{x}_i$ are the electron coordinates, and converts it into $N'=Nv(k/k_0)$ Slater determinants, each representing a certain one-electron excitation. N is the total number of electrons in the degenerate gas and the function $v(k/k_0)$ is given in I. For $k/k_0<1$, v is approximately $\frac{3}{4}(k/k_0)$. Let the Slater determinant in which momentum $\hbar\mathbf{k}_i$ has been excited to $\hbar\mathbf{k}_i+\hbar\mathbf{k}$ be designated by Ψ_i. The superposition generated by the scattering is therefore

$$\Psi=N'^{-\frac{1}{2}}\sum_i\Psi_i, \tag{1}$$

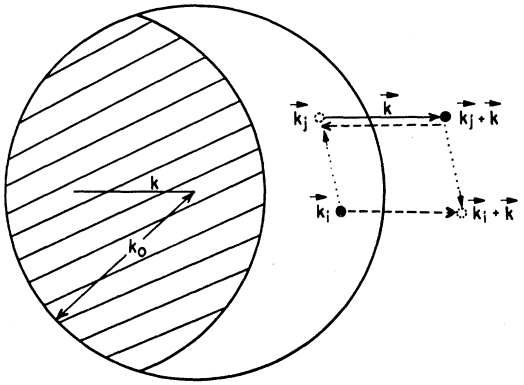

FIG. 1. Transfer of excitation between one-electron-excited configurations. The dashed line shows the interaction between the ith and jth electrons, while the dotted lines indicate the exchange transitions which are neglected here (but investigated in paper II). $\hbar\mathbf{k}$ is the momentum of excitation and $\hbar k_0$ the Fermi momentum. The shaded portion of the Fermi sea is prevented from contributing to the momentum-exciton by the Pauli exclusion principle.

and the potential energy we are interested in evaluating is

$$(\Psi,U\Psi)=N'^{-1}\sum_{ij}(\Psi_i,U\Psi_j), \tag{2}$$

where U is the total interaction operator,

$$U=\frac{4\pi e^2}{V}\sum_{k\neq 0}\frac{1}{k^2}\sum_{i<j}e^{i\mathbf{k}\cdot(\mathbf{x}_i-\mathbf{x}_j)}. \tag{3}$$

V is the volume of quantization and e the electron charge. The matrix element $(\Psi_i,U\Psi_j)$ is illustrated in Fig. 1. The solid line extending from the vacant circle labeled $\mathbf{k}_j$ to the dot labeled $\mathbf{k}_j+\mathbf{k}$ represents Ψ_j. Upon application of the operator U the electron of momentum $\hbar\mathbf{k}_j+\hbar\mathbf{k}$ is de-excited, as shown by the dashed line, and the electron of momentum $\hbar\mathbf{k}_i$ receives the excitation. The matrix element for the process is simply

$$M=(\Psi_i,U\Psi_j)=4\pi e^2/Vk^2, \tag{4}$$

independent of i and j, for $i\neq j$. Because of the identity of the electrons there is also an exchange contribution to M, as indicated by the dotted lines in Fig. 1. This complication does not, however, introduce any qualitatively new effects and will be ignored throughout the present paper. Its influence on the dispersion relation for plasma oscillations has been estimated in II and found to be relatively small. Substitution of Eq. (4) into Eq. (2) yields $(N'-1)M$, which can be replaced by $N'M$ because of the large value of N'. If we further make the substitution $N/V=k_0^3/3\pi^2$, we find

$$(\Psi,U\Psi)\approx\frac{e^2k_0}{\pi}\frac{k_0}{k}=\frac{1.22\ \text{ry}}{r_s}\frac{k_0}{k}. \tag{5}$$

As an example, consider the case $k/k_0=0.5$ for aluminum, where $r_s=2.07$. Substitution of the numbers

yields 16.0 ev, or more than ample to explain the relatively large magnitude of the energy loss. It is clear that this success is only qualitative, since for smaller values of the momentum transfer the potential energy of excitation becomes even larger, and approaches infinity as $k\rightarrow 0$. This result is, of course, incorrect. The error arises, as shown in Sec. IV, from the neglect of configurations containing more than one excited electron.

In order to better understand the nature of this large potential energy of excitation it is desirable to consider the positional correlation of the electrons. Because the Ψ of Eq. (1) is composed of more than one Slater determinant, or in other words is a mixture of configurations, there are important correlations in the positions of the electrons which are not present for the Ψ_i individually. Thus, the incident electron upon passing through the degenerate gas leaves the electrons in the state Ψ, in which they are "bunched." Because of this inhomogeneous charge distribution the total electrostatic potential energy is larger than for the unexcited Fermi sea. It is easily established from Eq. (1) that the pair distribution function is given by

$$P(\mathbf{x})=Nn+2nv(k/k_0)\cos(\mathbf{k}\cdot\mathbf{x}). \tag{6}$$

$P(\mathbf{x})d^3\mathbf{x}$ is the probability of finding one electron somewhere in volume V and a second within the infinitesimal volume $d^3\mathbf{x}$ at distance $\mathbf{x}$ from it. The quantity $n=N/V$ is the average electron density. Here again we have neglected exchange effects. Since the homogeneous term in $P(\mathbf{x})$ is cancelled by the positive background (we are replacing the ion lattice of the metal by the usual Sommerfeld model of a uniform fixed positive background), the total potential energy is given in terms of $P(x)$ by

$$(\Psi,U\Psi)=\frac{1}{2}\int\frac{e^2}{x}[P(\mathbf{x})-Nn]d^3\mathbf{x}. \tag{7}$$

Substitution from Eq. (6) and carrying out the integration yields the same results as in Eq. (5). Equation (7) makes it clear that the increased electrostatic energy in the excited state is directly attributable to the positional correlations. By taking these correlations into account, simply by considering a superposition rather than a single Slater determinant, it is possible to understand qualitatively the large magnitude of the energy loss.

III. ORIGIN OF THE DISCRETE STATE

The second of the two qualitative features of the experimental scattering data which are impossible to understand on the basis of noninteracting electrons is the sharpness of the eigenloss. This sharpness is incontrovertible evidence of excitation of a discrete state. Let us make the approximation of expanding Ψ, the wave function for this state, in terms of the one-electron excitations Ψ_i. Thus,

$$\Psi=\sum_i A_i\Psi_i, \tag{8}$$

where the sum is over $1\leq i\leq N'$. Let us further follow a sort of Tamm-Dancoff approach and neglect the portion of the interaction Hamiltonian which would take us outside the subspace of Hilbert space spanned by the basis states Ψ_i. If we introduce the abbreviations

$$T_i=E(\mathbf{k}_i+\mathbf{k})-E(\mathbf{k}_i), \tag{9}$$

and denote the energy of the excited state by E, the Schrödinger equation reads

$$T_iA_i+M\sum_j{}' A_j=EA_i. \tag{10}$$

The prime on the summation, which indicates that the term $j=i$ is excluded, can be dropped without appreciable error. The condition that the resulting set of homogeneous linear equations have a nontrivial solution is that the secular determinant should vanish. It is simpler, however, to put Eq. (10) into the form

$$A_i=\frac{M}{E-T_i}\sum_j A_j. \tag{11}$$

Summing over i and cancelling the common factors yields

$$F(E)\equiv M\sum_i(E-T_i)^{-1}=1. \tag{12}$$

The behavior of the function $F(E)$ is illustrated in Fig. 2, from which it is clear that Eq. (12) determines N' different eigenvalues for E. The lowest $N'-1$ of these are interspersed in the dense spectrum of the T_i, but the top eigenvalue is free to separate from the rest and rise to higher energy, provided the interaction matrix element M is sufficiently large. For very large values Eq. (12) requires $E\approx N'M$, which is just the case studied in Sec. II. As the interaction strength is reduced E drops toward the lower lying continuum and at a certain minimum strength coalesces with it. This

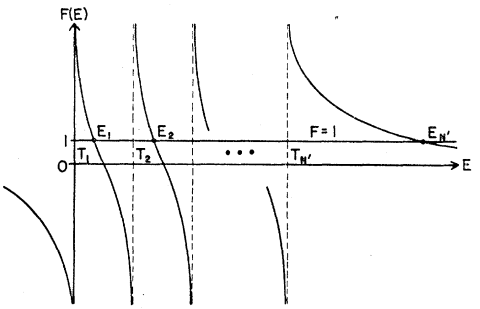

FIG. 2. $F(E)\equiv M\Sigma_i(E-T_i)^{-1}$ *vs* energy E. M is the matrix element of the Coulomb interaction for the transition indicated by the dashed lines of Fig. 1. T_i are the kinetic energy increments for the one-electron-excited configurations. The condition $F(E)=1$ determines the energy levels of the coupled system, in the Tamm-Dancoff approximation. All the eigenvalues except the highest must remain interspersed with the dense T_i spectrum. The highest eigenvalue splits off and forms the discrete momentum-exciton state, for sufficiently strong interaction.

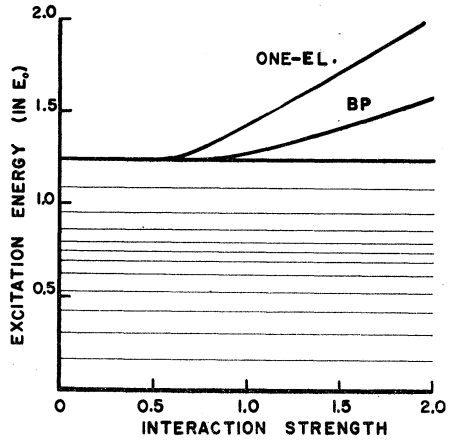

FIG. 3. Origin of the discrete state. Excitation energy (in units of the Fermi energy) *vs* the square of the electron charge, measured in units of its naturally occurring value. The abscissa value of 1.0 corresponds to the case found in nature. Passing to zero strength and neglecting the interaction of the electrons causes the discrete state to merge with the continuum and be lost. The spacing of the horizontal lines below excitation energy of $1.25E_0$ is inversely proportional to the density of energy levels in the continuum of one-electron excitations. The momentum of excitation is taken to be one-half the Fermi momentum. The upper curve shows the Tamm-Dancoff approximation to the excitation energy of the discrete state. Correction of the momentum-exciton model for correlation yields the lower curve, in complete agreement with the Bohm-Pines theory of plasma oscillations.

behavior has been calculated and is exhibited by the upper curve of Fig. 3. This figure is drawn for the case $k/k_0=\frac{1}{2}$ and the horizontal lines for excitation energies less than $1.25E_0$ indicate the dense T_i spectrum, or continuum, as we have been calling it. The density of the electron gas has been chosen as that corresponding to $r_s=2$, and the "interaction strength" is the ratio of the value of e^2 appearing in Eq. (3) to that actually occurring in nature. Since only the ratio of interaction energy to kinetic energy matters for a degenerate electron gas, one can alternatively keep e^2 at its naturally occurring value and vary the density. Thus, the abscissa can, with this interpretation, be considered equal to $r_s/2$.

The origin of the discrete state can be regarded as a manifestation of Hund's rule. In the absence of interaction the low-lying continuum of the T_i represents a set of essentially degenerate energy levels. "Turning on" the interaction splits the degeneracy and the linear combination of the basis states which has the highest spatial symmetry becomes the highest energy level. The wave function of Eq. (8) is essentially the same as that of Eq. (1), where all the expansion coefficients are equal and of the same sign. The other $N'-1$ linear combinations have expansion coefficients of both signs. Because of the much lower spatial symmetry of these energy levels they remain with the continuum.

IV. PLASMON AS A MOMENTUM-EXCITON

In Sec. II we have seen where the extra energy of excitation comes from, while in Sec. III we have studied how the interaction produces a discrete excited state of the electron plasma. Having removed these two qualitative discrepancies, we are now interested in seeing how well we can expect our simple quantum-mechanical approach to describe quantitatively the sharp eigenloss. A particularly convenient check is provided by the Nozières-Pines sum rule. According to Eq. (52) of II, the oscillator strength corresponding to excitation of Ψ of Eq. (8) above is restricted by the inequality

$$f_{10}{}^{\mathbf{k}}\leq N. \tag{13}$$

If we continue to use the simple Fermi-sea description for the ground state, we find

$$|V(\rho_{\mathbf{k}})_{10}|^2=|\textstyle\sum_i A_i|^2=\left[\sum_i \dfrac{M^2}{(E-T_i)^2}\right]^{-1}. \tag{14}$$

Here we have squared Eq. (11) and applied the requirement of normalization. Let us consider the case where the discrete state is well separated from the continuum, so we can write

$$E-T_i\approx E\approx(\Psi,U\Psi)\approx N'M. \tag{15}$$

Equation (14) becomes simply N'^2, which, when substituted into Eq. (53) of II, yields

$$\begin{aligned} f_{10}{}^{\mathbf{k}}&\approx N\frac{8\pi mne^2}{\hbar^2k^4}v^2(k/k_0)\\ &\approx N\frac{3}{2\pi}(k_0a_0)^{-1}\left(\frac{k_0}{k}\right)^2\\ &=N(0.498r_s^{\frac{1}{2}}k_0/k)^2. \end{aligned} \tag{16}$$

According to Sec. IV of II, the quantity in parentheses in the last form of Eq. (16) is of the order of unity in the vicinity of the cutoff. Although the approximations made in deriving Eq. (16) are not valid in this case, it is clear that Eq. (16) is compatible with the requirement of Eq. (13). This is not the case for smaller values of k, however, for which Eq. (16) yields $f_{10}{}^{\mathbf{k}}>N$, definitely inconsistent with Eq. (13). Thus, our simple theory grossly overestimates the oscillator strength of the momentum-exciton for small momenta of excitation.

This failure of our one-electron excitation theory can be expected to extend to other quantities of interest. A refinement of the theory is clearly required before it can be used for quantitative purposes. The error is due to the Tamm-Dancoff approximation of restricting the excited state wave function to the one-electron subspace of Hilbert space. In reality the interaction couples this subspace to the states of three-, five-, etc., electron excitation. In addition, it is clear that whenever the interaction is strong enough to cause the discrete state to split off from the continuum, it will also introduce important correlations into the ground state. These correlations are described by admixtures of two-, four-,

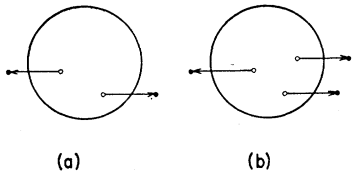

FIG. 4. Higher configurations which, as admixtures, represent positional correlations in the stationary states of an interacting degenerate electron gas. Diagram (a) shows a two-electron admixture in the ground state while (b) shows a typical three-electron excitation which occurs as an admixture in the excited state.

etc., electron excitations. A typical two-electron ground state admixture is shown in Fig. 4(a), while Fig. 4(b) shows a three-electron admixture in the excited state. It would be a difficult problem to calculate separately the energies of the ground state and excited state, taking into account accurately the correlations. Fortunately this is not necessary here, for we are interested only in the difference of these two energies, which is much more easily calculated. The calculation is facilitated by Feynman's time-dependent formulation[1] of the Schrödinger equation. As illustrated in Fig. 4(a), the excitations which represent the ground state correlations are created and annihilated in pairs. The graphs which determine the ground-state energy consist therefore of closed loops, or "bubbles." These bubbles also appear in the excited-state graphs. Calculating the excitation energy by taking the difference cancels out the bubbles and leaves only the connected graphs of Fig. 5. Figure 5(a) shows an interaction taking place at time 1 so that the excitation is transferred from a certain one-electron excited configuration to another. At time 2 a second interaction takes place and the excitation is passed on to yet another configuration. The flow of time is upward and the excited configuration of an electron outside the Fermi sea plus the hole left behind is represented by a single line. This type of graph has already been taken into account in Sec. III. Figure 5(b), on the other hand, illustrates the refinement necessary in the momentum-exciton model to make it give quantitatively correct results. The interaction which takes place at time 2 creates an excitation-pair, resulting in a three-electron admixture in the excited-state wave function. The member of the pair which carries the arrow pointed backwards in time corresponds to the excitation of the left hand side of Fig. 4(b). It carries momentum $-\hbar\mathbf{k}$ and, by virtue of the interaction at time 1 (later than time 2), annihilates with the incoming one-electron excitation. It is convenient to assign backward-pointing arrows to the excitations of momentum $-\hbar\mathbf{k}$ so as to emphasize that the excitation can be considered to be conserved and to be carried continuously along its "world-line." The world-line can make an arbitrary number of "jogs" backwards in time as it works its way from the past to the future.

[1] R. P. Feynman, Phys. Rev. **76**, 749 (1949).

Let $A_i^{(\pm)}\exp(-iEt/\hbar)$ denote the probability amplitudes at time t of the forward- and backward-going parts of the graphs of Fig. 5. According to the Schrödinger equation in the interaction representation, the increment in the amplitudes due to the interaction acting during the infinitesimal period dt_1 at time t_1 is

$$-(idt_1/\hbar)\textstyle\sum_j(A_j^{(+)}+A_j^{(-)})\exp(-iEt_1/\hbar).$$

The propagation of the forward-going excitation from time t_1 to the later time t_2 is described by the propagator

$$\exp\{-i[E(\mathbf{k}_i+\mathbf{k})-E(\mathbf{k}_i)](t_2-t_1)/\hbar\}.$$

The forward-going amplitude at $t=0$ is therefore

$$\begin{aligned}A_i^{(+)}&=-i\hbar^{-1}M\sum_j(A_j^{(+)}+A_j^{(-)})\int_{-\infty}^{0}\exp(-iEt_1/\hbar)\\&\quad\times\exp\{i[E(\mathbf{k}_i+\mathbf{k})-E(\mathbf{k}_i)]t_1/\hbar\}dt_1\\&=\frac{M}{E-E(\mathbf{k}_i+\mathbf{k})+E(\mathbf{k}_i)}\sum_i(A_j^{(+)}+A_j^{(-)}).\end{aligned}\tag{17}$$

Except for the presence of $A_j^{(-)}$ this equation is identical to Eq. (11). The propagation from t_1 to $t_2<t_1$ is, on the other hand, described by the propagator

$$\exp\{-i[E(\mathbf{k}_i-\mathbf{k})-E(\mathbf{k}_i)](t_1-t_2)/\hbar\}.$$

The backward-going amplitude at $t=0$ is therefore

$$\begin{aligned}A_i^{(-)}&=-i\hbar^{-1}M\sum_j(A_j^{(+)}+A_j^{(-)})\int_{0}^{\infty}\exp(-iEt_1/\hbar)\\&\quad\times\exp\{-i[E(\mathbf{k}_i-\mathbf{k})-E(\mathbf{k}_i)]t_1/\hbar\}dt_1\\&=\frac{M}{-E-E(\mathbf{k}_i-\mathbf{k})+E(\mathbf{k}_i)}\sum_i(A_j^{(+)}+A_j^{(-)}).\end{aligned}\tag{18}$$

Equations (17) and (18) are identical to Eq. (30) of II [after substituting there from Eq. (7)]. Since the Bohm-Pines dispersion relation follows from these equations, they complete the identification of the momentum-exciton with the plasmon. To illustrate the quantitative, as distinguished from qualitative, nature of the refinement of the present section, the Bohm-Pines plasmon energy has been included for comparison in Fig. 3 (lower curve).

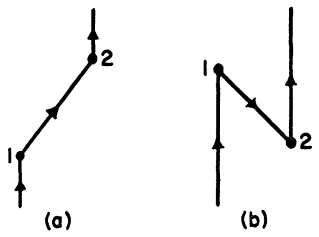

FIG. 5. Feynman graphs basic to the momentum-exciton model. Graphs of type (a), in which the excitation is always carried forward in time, are already taken into account by the Tamm-Dancoff approximation. (The flow of time is upward.) Inclusion of graphs of type (b) corrects for correlation and completes the identification of the momentum-exciton with the Bohm-Pines plasmon.

The inclusion of Feynman graphs with backward-going parts not only corrects the excitation energy but removes the difficulty with the oscillator strength as well. The square of the matrix element for plasma excitation is simply

$$|V(\rho_{\mathbf{k}})_{10}|^2=|\sum_j(A_j^{(+)}+A_j^{(-)})|^2$$
$$=\sum_i(|A_i^{(+)}|^2-|A_i^{(-)}|^2)$$
$$\times\left\{\sum_i\frac{M^2}{[E-E(\mathbf{k}_i+\mathbf{k})+E(\mathbf{k}_i)]^2}\right.$$
$$\left.-\sum_i\frac{M^2}{[-E-E(\mathbf{k}_i-\mathbf{k})+E(\mathbf{k}_i)]^2}\right\}^{-1}. \quad (19)$$

Use has been made of Eqs. (17) and (18). Normalization to unit temporal flow of excitation requires

$$\sum_i(|A_i^{(+)}|^2-|A_i^{(-)}|^2)=1. \quad (20)$$

Introducing the reduction factor G^{-1} of II [following Eq. (33)] leads to

$$|V(\rho_{\mathbf{k}})_{10}|^2=V\frac{k^2\hbar\omega_p}{8\pi e^2}G^{-1}, \quad (21)$$

in exact agreement with Sec. V of II.[2]

[2] In the general identification of the work of the present paper with that of II it should be noted that $A_i^{(-)}$, although in actuality real, is formally the complex conjugate of the corresponding quantity in II. It should also be mentioned that all of the sums in the present work are restricted by the Pauli exclusion principle. This restriction has, however, no practical effect, as proved in the discussion following Eq. (32).

V. SUMMARY

In the above work it has been shown that a straightforward quantum-mechanical treatment of the excitation of a degenerate electron gas automatically yields the two characteristic qualitative features of collective plasma oscillations, provided only that the interaction of the electrons is taken into account. In Sec. IV the additional refinement is presented which makes the momentum-exciton model quantitatively useful and which completes the identification of the momentum-exciton with the plasmon. The plasmon oscillator strength as well as excitation energy is worked out, thereby supplanting the derivations of the previous paper, which invoked the *correspondence principle*. The present work also makes it clear why the continuum is not excited by small-angle scattering of the incident electrons. The continuum states have low spatial symmetry and do not exhibit the bunching found in the discrete state. There is consequently hardly any electrostatic field associated with these excitations, and they are coupled only very weakly with the incident electrons. It is possible to show that the present theory is equivalent to the screening out by the conduction electrons of the external field set up by the incident electrons, where the screening is calculated by Lindhard's[3] and Hubbard's[4] theory of the dielectric constant. It is hoped to deal more with the excitation of the continuum in the future.

[3] J. Lindhard, Kgl. Danske Videnskab. Selskab, Mat.-fys. Medd. **28**, No. 8 (1954).

[4] J. Hubbard, Proc. Phys. Soc. (London) **A68**, 441, 976 (1955).